ELSEVIER

Journal of Crystal Growth 149 (1995) 131–140

JOURNAL OF CRYSTAL GROWTH

Onset of double-diffusive convection of unidirectionally solidifying binary solution with variable viscosity

Jay W. Lu , Falin Chen *

Institute of Applied Mechanics, National Taiwan University, Taipei, Taiwan 10764, ROC

Received 21 July 1994; manuscript received in final form 22 December 1994

Abstract

As a metallic melt solidifies, the viscosity variation may dramatically influence the convection induced by solidification as well as the microstructure of the resultant casting. In the present paper, we study the effect due to viscosity variation on the onset of double-diffusive convection occurring during the directional solidification of a binary solution cooling from below. Results show that as the viscosity contrast, denoted by γ in Eq. (14), increases the stability of convection is enhanced and the mode of convection can change from the mushy-layer mode into the boundary-layer mode. The critical Rayleigh number R_m^c, for both the mushy-layer and boundary-layer modes, increases exponentially with γ for all the parameter ranges considered, in contrast to the thermal convection case in which the critical Rayleigh number increases linearly with γ. This difference emerges mainly from the length scale of the convection layer, which is of solutal boundary-layer thickness in the present study and is of thermal boundary-layer thickness in the thermal convection case.

1. Introduction

Directional solidification is one of the most important advanced processing techniques for metallurgists to create and exploit exceptionally strong alloys with increased creep rupture strain and improved thermal fatigue behavior, two important characteristics for modern turbine blades [1]. Under some circumstances, however, defects known as freckles form in the casting. Their presence causes a deleterious effect on the mechanical properties of the castings. The formation of freckles has been extensively studied in an analogous system, the aqueous ammonium chloride solution cooling from below, by several investigators [2–6]. They found that a dendritic mushy-zone forms between the bulk fluid and the eutectic solid. The gradients of temperature and solute that necessarily occur in the solidifying system destabilize the nominally motionless basic state, leading to the onset of double-diffusive convection. The convection is largely confined to the solutal boundary-layer above the melt/mush interface (a boundary-layer mode convection) while the fluid in the mush does not participate in the initial instability [3,4]. As crystallization evolves, the double-diffusive convection becomes more intense, inducing a subcritical mushy-layer mode convection, a convection circulating between the fluid and mushy regions [6,7]. It is this subcritical instability that gives way to the occurrence of plume convection and the formation of freckles. The double-diffusive convection is therefore closely related to the formation of freckles.

The onset of double-diffusive convection of a binary solution cooling from below has been investi-

* Corresponding author.

SSDI 0022-0248(94)01006-4

gated both theoretically and experimentally [3–6]. It is found that the stability characteristics are influenced by several physical parameters. The viscosity variation, nevertheless, is especially important for the metallic alloy, which, however, has not yet been considered. In fact, the viscosity-variation changes widely depending on the alloys considered. For example, the viscosity of glass forming alloys can increase by $O(10^{20})$ when the temperature decreases from working condition to melting point [8], whereas for lead–tin alloys the viscosity varies by a factor of two as the temperature changes over 200 K [9]. Since in the thermal convection case [10,11] the viscosity variation due to temperature change significantly influences the convective instability, we thus expect that the temperature-dependent viscosity is also influential on the double-diffusive convection. In the present study, accordingly, we investigate the variable-viscosity effect on the onset of double-diffusive convection in directionally solidifying binary solutions. Emphasis is placed on the effect of viscosity variation on both the stability criteria and the convection mode. A wide range of physical parameters, such as the Lewis number ϵ, the Prandtl number σ, and the buoyancy ratio $\mathcal{A}$ (see definitions in Section 2), is considered.

2. Mathematical formulation

Consider a binary solution of concentration C_∞ ($> C_E$) and temperature T_∞ with temperature-dependent viscosity unidirectionally solidifying from below, where C_E is the eutectic concentration of the solution. For a solution of $C_\infty > C_E$, the ejected fluid due to solidification is of less concentration than the bulk fluid. As a result, the fluid at below is of less concentration and low temperature, forming vertical gradients of temperature and concentration, giving way to destabilizing the nominally motionless basic state and leading to the onset of double-diffusive convection. Assume the eutectic front is morphologically unstable [12], a dendritic mushy region forms between the eutectic solid region and the semi-infinite fluid region. Both the solid/mush and the mush/fluid interfaces are assumed moving upwards with a constant velocity V. Two sets of equations govern the fluid motion of the system. Each set consists of the conservation of mass, momentum, heat, and solute. The density of the fluid is assumed to be constant except in the gravity term, in which the density is a function of temperature and concentration. The viscosity of the fluid is considered as an exponential function of temperature

$$\mu^* = \mu_0 \exp[-c(T - T_\infty)], \tag{1}$$

where $c > 0$ is an arbitrary constant, indicating that the viscosity of the fluid decreases with increasing temperature, and $\mu_0 = \nu_0 \rho_0$ is the reference dynamic viscosity, ρ_0 is the reference density, and ν_0 is the reference kinematic viscosity. The exponential form of viscosity–temperature relation is suitable for an aqueous solution [10], on which we will focus in the present paper. Other relations are also available, such as the Arrhenius form $\mu^* = C \exp(c/T)$ [9], the Litovitz form $\mu^* = A \exp(a/T^3)$ [13] and some other more complicated forms [14] may be used for other alloys. In above forms, C, c, A, a are constants determined experimentally.

We nondimensionalize the fluid velocities with the interface velocity V, distances with κ_{tl}/V, time with κ_{tl}/V^2, viscosity with μ_0, and pressure with $\beta \Delta C \rho_0 g \kappa_{tl}/V$, in which κ_{tl} is the thermal diffusivity of the fluid, $\beta = \beta^* - \Gamma\alpha^*$, β^* and α^* are solutal and thermal expansion coefficients, respectively, Γ is the slope of the liquidus curve, which is assumed to be a constant, $\Delta C = C_\infty - C_E$, and g is the gravitational acceleration. By assuming the physical properties of the fluid and solid to be identical and by taking the Galilean transformation with respect to the moving interface, we obtain the following dimensionless equations. In the fluid region $h < z < \infty$, we have

$$\nabla \cdot \boldsymbol{u} = 0, \tag{2}$$

$$\left(\frac{\partial}{\partial t} - \frac{\partial}{\partial z}\right)\theta + \boldsymbol{u} \cdot \nabla\theta = \nabla^2\theta, \tag{3}$$

$$\left(\frac{\partial}{\partial t} - \frac{\partial}{\partial z}\right)\Theta + \boldsymbol{u} \cdot \nabla\Theta = \epsilon\nabla^2\Theta, \tag{4}$$

$$\frac{1}{\sigma}\left[\left(\frac{\partial}{\partial t} - \frac{\partial}{\partial z}\right) + \boldsymbol{u} \cdot \nabla\right]\boldsymbol{u} = \nabla \cdot (\mu D) + R_T\theta\boldsymbol{e}_k - R_C\left(\Theta\boldsymbol{e}_k + \frac{\beta}{\beta^*}\nabla p\right), \tag{5}$$

where $\boldsymbol{u} = (u, v, w)$ is the velocity vector in Cartesian coordinates, $D = \nabla\boldsymbol{u} + \nabla\boldsymbol{u}^{\mathrm{T}}$ is the deviatoric strain tensor and the superscript T denotes the transverse of the tensor, the dimensionless temperature and concentration are defined as

$$\theta = \frac{T - T_{\mathrm{L}}(C_\infty)}{\Delta T}, \quad \Theta = \frac{C - C_\infty}{\Delta C}, \tag{6}$$

where $\Delta T = \Gamma\Delta C = T_{\mathrm{L}}(C_\infty) - T_{\mathrm{E}}$, $T_{\mathrm{L}}(C_\infty)$ is the liquidus temperature corresponding to C_∞, $\epsilon = \kappa_{\mathrm{cl}}/\kappa_{\mathrm{tl}}$ is the Lewis number, κ_{cl} is the solutal diffusivity of the fluid, $\sigma = \nu/\kappa_{\mathrm{tl}}$ is the Prandtl number, $\boldsymbol{e}_k$ is the unit vector in the vertical direction, p is the pressure, R_{T} and R_{C} are thermal and solutal Rayleigh numbers given by

$$R_{\mathrm{T}} = \frac{g\alpha^*\Delta T H^3}{\kappa_{\mathrm{tl}}\nu_0}, \quad R_{\mathrm{C}} = \frac{g\beta^*\Delta C H^3}{\kappa_{\mathrm{tl}}\nu_0}, \tag{7}$$

where $H = \kappa_{\mathrm{tl}}/V$ is the characteristic length. In the mushy region $0 < z < h$, we have

$$\nabla \cdot \boldsymbol{u} = 0, \tag{8}$$

$$\left(\frac{\partial}{\partial t} - \frac{\partial}{\partial z}\right)\theta + \boldsymbol{u}\cdot\nabla\theta = \nabla^2\theta - \mathcal{F}\left(\frac{\partial}{\partial t} - \frac{\partial}{\partial z}\right)\chi, \tag{9}$$

$$\chi\left(\frac{\partial}{\partial t} - \frac{\partial}{\partial z}\right)\Theta + \boldsymbol{u}\cdot\nabla\Theta = -(\Theta - \mathcal{C})\left(\frac{\partial}{\partial t} - \frac{\partial}{\partial z}\right)\chi, \tag{10}$$

$$\frac{\mu\boldsymbol{u}}{\Pi(\chi)} = -R_{\mathrm{m}}(\nabla p + \theta\boldsymbol{e}_k), \tag{11}$$

where χ is the porosity, $\mathcal{C} = (C_{\mathrm{S}} - C_\infty)/\Delta C$ is the concentration ratio, C_{S} is the concentration of solid, $\mathcal{F} = \mathcal{L}/c_{\mathrm{p}}\Delta T$ is the Stefan number, $\mathcal{L}$ is the latent heat of fusion, c_{p} is the specific heat, and R_{m} is the Rayleigh number for the mushy layer given as

$$R_{\mathrm{m}} = \frac{g\beta\Delta C\Pi_0 H}{\kappa_{\mathrm{tl}}\nu_0}, \tag{12}$$

in which Π_0 is the reference permeability. The dimensionless viscosity function μ is written as

$$\mu = \exp\left(\gamma\frac{\theta_\infty - \theta_{\mathrm{b}}}{\theta_\infty - \theta_{\mathrm{E}}}\right), \tag{13}$$

where

$$\gamma = \ln\left(\frac{\mu_{\mathrm{E}}}{\mu_\infty}\right) \tag{14}$$

accounts for the viscosity contrast between the fluid at the eutectic front and the bulk fluid at infinity, and θ_{b} is the dimensionless basic state temperature. The dimensionless permeability function $\Pi(\chi)$ is an arbitrary function of the porosity χ, which we assume to be uniform as $\Pi(\chi) = 1$ [5] in the present study. Note that since the thermodynamic equilibrium condition holds in the mushy layer [6], the liquidus relation $\theta = \Theta$ is applied in the mushy layer. Note also that since the solute diffusion in the mush is so small, we assume ϵ in the mush to be zero.

The boundary conditions at $z \to \infty$ are

$$\theta \to \theta_\infty, \tag{15a}$$

$$\Theta \to 0, \tag{15b}$$

$$\boldsymbol{u} \to 0, \tag{15c}$$

at the melt/mush interface $z = h$ they are

$$\theta = \Theta, \tag{16a}$$

$$\boldsymbol{n}\cdot\nabla\theta = \boldsymbol{n}\cdot\nabla\Theta, \tag{16b}$$

$$[\boldsymbol{n}\cdot\boldsymbol{u}] = 0, \tag{16c}$$

$$[\theta] = 0, \tag{16d}$$

$$[\boldsymbol{n}\cdot\nabla\theta] = 0, \tag{16e}$$

$$\chi = 1, \tag{16f}$$

$$[\sigma_{\mathrm{n}}] = 0, \tag{16g}$$

$$\left.\frac{\partial u_2}{\partial z}\right|_{h+} = \Lambda\sqrt{\frac{\mathcal{H}}{\Pi(1)}}(u_2|_{h+} - u_2|_{h-}), \tag{16h}$$

where the square brackets denote the jump of the enclosed quantity across the interface, $\boldsymbol{n}$ is a unit vector

normal to the interface, $\mathcal{H} = H^2/\Pi_0$, σ_n is the normal stress, and $\boldsymbol{u}_2$ is the plane velocity vector (u, v). The physical meaning of above boundary conditions Eqs. (16a)–(16g) is provided by Chen et al. [6]. Eq. (16h) is the Beavers–Joseph boundary condition accounting for the velocity difference across the interface [15]. Note that the constant Λ of Eq. (16h) is determined experimentally to be $0.1 \leq \Lambda \leq 4$, and we assume $\Lambda = 0.1$ in the present study. The interface position h is determined to be a part of the solution. At the mush/solid interface $z = 0$ we have

$$\theta = -1, \tag{17a}$$

$$w = 0, \tag{17b}$$

where $T = T_E$ is assumed and the vertical velocity vanishes.

3. Small disturbance equations and method of solution

Since the viscosity does not play a role in determining the basic state, the present motionless basic state is therefore the same as that of Worster [5], in which a constant viscosity is considered. We linearize the equations of Section 2 by introducing small disturbances to the basic state quantities and substituting their combination into the original equations. After obtaining the linearized equations and introducing normal modes proportional to $\exp(\omega t + i\alpha x)$, the small disturbance equations are as follows. In the fluid region, we have

$$(D^2 - \alpha^2)W = \Omega, \tag{18}$$

$$\left(D^2 + D - \omega - \alpha^2\right)\theta = \theta_b' W, \tag{19}$$

$$\left(\epsilon D^2 + D - \omega - \epsilon\alpha^2\right)\Theta = \Theta_b' W, \tag{20}$$

$$\left[\mu(D^2 - \alpha^2) + \frac{D - \omega}{\sigma} + 2\mu' D\right]\Omega + \mu''(\Omega + 2\alpha^2 W) = \alpha^2[R_T\theta - R_C\Theta]. \tag{21}$$

In these equations, the notations W, θ, Θ now represent small disturbance quantities. In addition, both $'$ and D represent the vertical derivative $\mathrm{d}/\mathrm{d}z$, α is the horizontal wave number, ω is the normal mode frequency, and Ω is the disturbance vorticity.

Similarly, in the mushy region we have

$$(D^2 + D - \omega - \alpha^2)\theta + \mathcal{F}(D - \omega)\chi = \theta_b' W, \tag{22}$$

$$[\chi_b(D - \omega) + \chi_b']\theta + [(\theta_b - C)(D - \omega) + \theta_b']\chi = \theta_b' W, \tag{23}$$

$$[f(D^2 - \alpha^2) + f'D]W = \alpha^2 R_m\theta, \tag{24}$$

where $f = \mu/\Pi(\chi_b)$. Note that in Eq. (23) the liquidus relation $\theta = \Theta$ has been applied. The Rayleigh numbers in the fluid can be replaced by the Rayleigh number in the mush by the relations $R_T = \mathcal{A}\mathcal{H}R_m$ and $R_C = (1 + \mathcal{A})\mathcal{H}R_m$, where $\mathcal{A} = \Gamma\alpha^*/\beta$ is the buoyancy ratio between the buoyancy due to temperature to that due to concentration.

The boundary conditions at $z \to \infty$ are

$$\theta = 0, \tag{25a}$$

$$\Theta = 0, \tag{25b}$$

$$W = 0, \tag{25c}$$

$$DW = 0, \tag{25d}$$

at $z = h$ they are

$$\theta = \Theta, \tag{26a}$$

$$D\Theta - D\theta = \left(\frac{1 - \epsilon}{\epsilon}\right)\theta_b'\eta, \tag{26b}$$

$$[W] = 0, \tag{26c}$$

$$[\theta] = 0, \tag{26d}$$

$$[D\theta] = -\frac{\mathcal{F}\theta_b'}{C - \theta_i}\eta, \tag{26e}$$

$$\chi = \frac{\theta_b'}{\theta_i - C}\eta, \tag{26f}$$

$$DW|_{h-} = -\frac{\Pi(1)}{\mathcal{H}\mu}\left[-\frac{1}{\sigma}(\omega - D)DW + \mu'(D^2 + \alpha^2)W + \mu D\Omega - 2\mu\alpha^2 DW\right]_{h+}, \quad (26g)$$

$$D^2W|_{h+} = \alpha\sqrt{\frac{\mathcal{H}}{\Pi(1)}}(DW|_{h+} - DW|_{h-}), \quad (26h)$$

and at $z = 0$ they are

$$\theta = 0, \quad (27a)$$

$$W = 0, \quad (27b)$$

where η is the small perturbation of the interface position. Eqs. (18)–(27) consist of a complex eigenvalue problem

$$F(R_m, \alpha, \omega; \theta_\infty, \mathcal{C}, \mathcal{A}, \epsilon, \sigma, \mathcal{F}, \mathcal{H}, \gamma) = 0, \quad (28)$$

having totally 13 orders of differential equations along with 14 boundary conditions, in which Eq. (26b) is employed to solve the disturbance melt/mush interface position η. We solve this complex eigenvalue problem with a shooting method. For details of the numerical method the reader is referred to Chen et al. [6].

4. Numerical results

The case of $\mathcal{C} = \mathcal{F} = \theta_\infty = 1$, $\sigma = 10$, $\epsilon = 0.025$, $\mathcal{A} = 0.5$, $\mathcal{H} = 10^5$, and a uniform permeability $\Pi(\chi) = 1$ is considered, which is relevant to aqueous solutions [6]. We focus on the variable viscosity effect on the stability characteristics of the double-diffusive convection. Other values of ϵ, σ, and $\mathcal{A}$ are also considered. As the effect of one parameter is considered, the values of other parameters are fixed as shown above.

Fig. 1 illustrates the neutral curve topology of the aqueous solution of four different γ. In Fig. 1a, the viscosity is constant ($\gamma = 0$), the neutral curve consists of three monotonic branches (solid curves) and three oscillatory branches (dotted curves). For the monotonic branches, the corresponding convection mode is steady in nature. The left branch corresponds to the mushy-layer mode convection, a convection circulating in both the fluid- and mushy-layer (see Fig. 2a for the most critical mode on the branch). The right branch corresponds to the boundary-layer mode convection, a convection largely confined to the solutal boundary layer above the melt/mush interface (see Fig. 2d for the most critical mode on the branch). The top branch sitting well above the other two branches is of much larger stability. For the oscillatory branches, there is a Hopf bifurcation branch connecting the right and the left monotonic branches, the corresponding oscillation frequency ω_i is shown with the dashed curve below the branch. Another oscillatory branch emerges from the upper part of the right monotonic branch and penetrates through the same branch into another domain. The frequency of this branch is generally larger than that of the connecting branch. The third oscillatory branch is also a connecting branch sitting between the top and the right monotonic branches with low frequency.

From Fig. 1a it is seen that the boundary-layer mode convection is the most unstable mode, the onset of convection is therefore largely confined to the compositional boundary layer above the melt/mush interface (Fig. 2d). For $\gamma = 2$ (Fig. 1b), the viscosity at the eutectic solid boundary is larger than that of the bulk fluid, the left monotonic branch moves upwards, indicating that the mushy-layer mode becomes more stable. It can be seen from Fig. 2b that the onset of convection in the mushy-layer is diminishing since the viscosity in the mush increases. As γ increases further, see Fig. 1c for $\gamma = 4$, the mushy-layer mode becomes increasingly stable compared with the boundary-layer mode. For $\gamma = 8$ (Fig. 1d), the mushy-layer mode virtually vanishes and the boundary-layer mode predominates.

Although the onset flow pattern of boundary-layer mode is hardly influenced by the value of γ (see Figs. 2d–2f), the critical Rayleigh number R_m^c, nevertheless, increases with γ by the relation $\log(R_m^c) \propto \gamma$. Figs. 3a and 3b show R_m^c and α^c versus γ for $\epsilon = 0.01$, 0.025 and 0.1, respectively. For $\epsilon = 0.01$, the mushy-layer mode convection predominates when $\gamma < \gamma^c = 3.82$ and the boundary-layer mode becomes most unstable otherwise. Fig. 4 demonstrates examples of these two critical modes, showing that the mushy-layer mode consists of two separated cells coupled viscously in the vicinity of the melt/mush in-

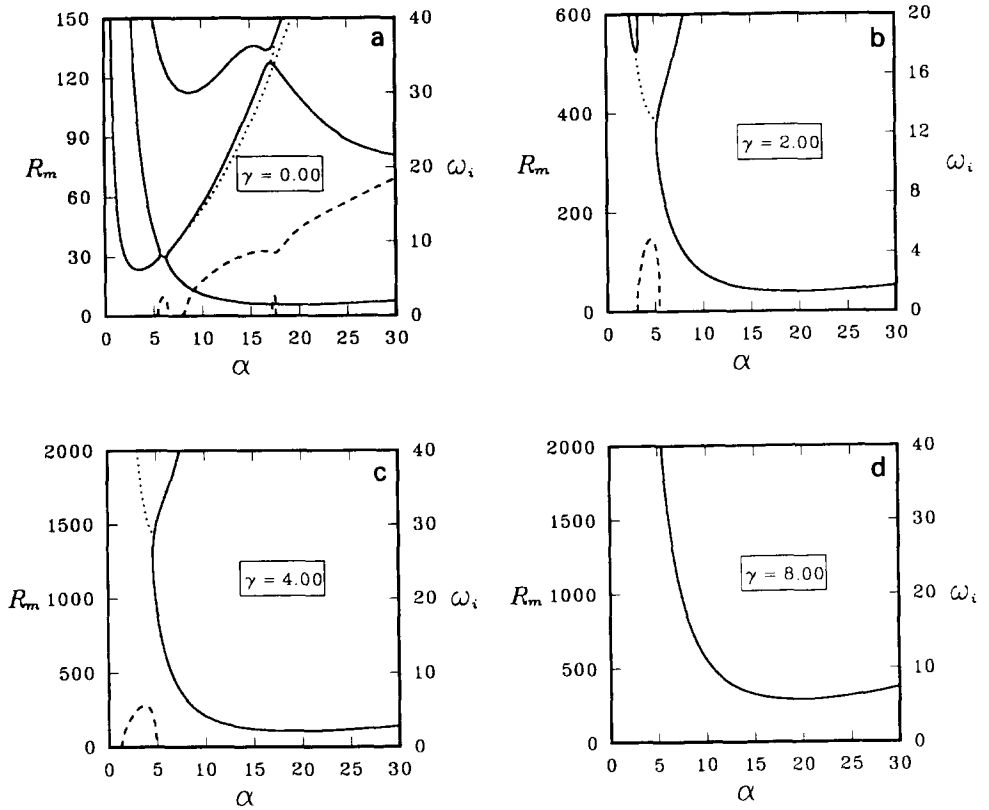

Fig. 1. Topology of the neutral curves (solid: monotonic mode; dot: oscillatory mode) and frequency ω_i (dash) of the oscillatory mode convection for various γ. (a) $\gamma = 0$; (b) $\gamma = 2$; (c) $\gamma = 4$; (d) $\gamma = 8$.

terface, and that the boundary layer mode is of much smaller wavelength and is largely confined to the boundary-layer above the interface. For both modes, $\log(R_m^c)$ increases linearly with γ. For other ϵ, this linear relation between $\log(R_m^c)$ and γ also holds and the onset of convection is of boundary-layer mode. A detailed discussion of the physical meaning of the ϵ-effect for $\gamma = 0$ is available in the paper of Chen et al. [6], which is helpful to explain the present results of $\gamma \neq 0$ and is briefly stated in the following.

Physically, a larger ϵ implies a thicker compositional boundary-layer above the melt/mush interface, providing a larger space for the fluid to convect and thus a less stable state for the boundary-layer mode [6]. This explains why the R_m^c of the boundary-layer mode in Fig. 3a decreases with increasing ϵ. As the viscosity-variation becomes effective ($\gamma > 0$), the stability of the boundary-layer mode increases with γ due to increasing viscosity. The wave length (or α^{-1}), however, is hardly influenced by γ because the thickness of the compositional boundary-layer, to which the convection cell is largely confined, virtually does not change with γ. For the case of $\epsilon = 0.01$, the onset of convection is of mushy-layer mode when γ is small. As γ increases up to $\gamma^c = 3.82$ and larger, the larger viscosity at below retards the convection in the mush, resulting in the occurrence of the boundary-layer mode. It is noted that γ^c increases with decreasing ϵ, namely, for liquid metals whose ϵ is usually smaller than 0.01, the onset of the convection in the large range of γ is of the mushy-layer mode. Since the emphasis of the present paper is placed on the mode-competition between boundary-layer and mushy-layer modes, which the case of $\epsilon = 0.01$ has illustrated clearly, we thus has

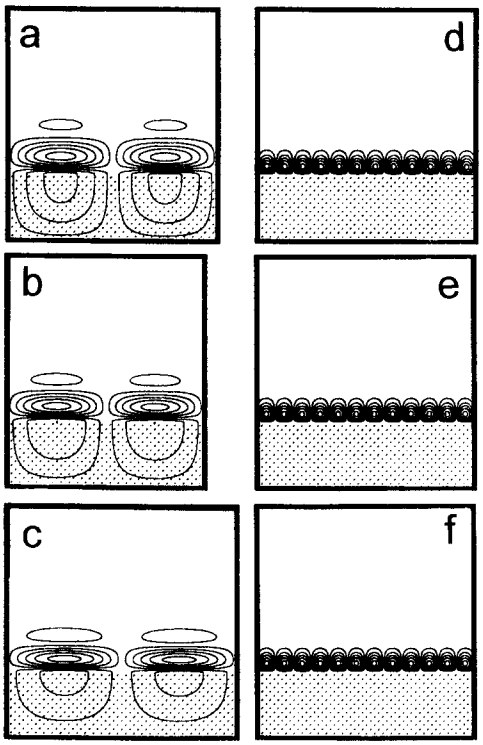

Fig. 2. Onset streamline pattern corresponding to the most critical mode of Fig. 1, in which (a–c) are the mushy-layer mode convection and (d–f) are the boundary-layer mode convection. (a) $\gamma = 0$, $R_m = 23.59$, $\alpha = 3.42$; (b) $\gamma = 2$, $R_m = 104.8$, $\alpha = 3.63$; (c) $\gamma = 4$, $R_m = 524.1$, $\alpha = 3.11$; (d) $\gamma = 0$, $R_m = 5.647$, $\alpha = 19.42$; (e) $\gamma = 2$, $R_m = 15.03$, $\alpha = 19.50$; (f) $\gamma = 4$, $R_m = 40.05$, $\alpha = 19.54$. (Note that the shaded region accounts for the mushy-layer. The wavelength is scaled with respect to the mushy-layer height. The same applies to Fig. 4.)

no attempt to investigate the cases of $\epsilon < 0.01$.

The linear relation between $\log(R_m^c)$ and γ can become obvious if rescaling is considered. The proper scale can be obtained by considering the local behavior of the instability, similar to the analyses in the thermal convection case with a variable viscosity fluid [10,11]. Since in the present problem the onset of the convection is mostly largely confined to the compositional boundary layer above the melt/mush interface, we consider a local Rayleigh number defined as

$$R_{loc} = \frac{g\beta^* \Delta C_{z^*} H^3}{\kappa_{tl} \nu_{z^*}} \tag{29}$$

for the boundary-layer mode convection. In Eq. (29),

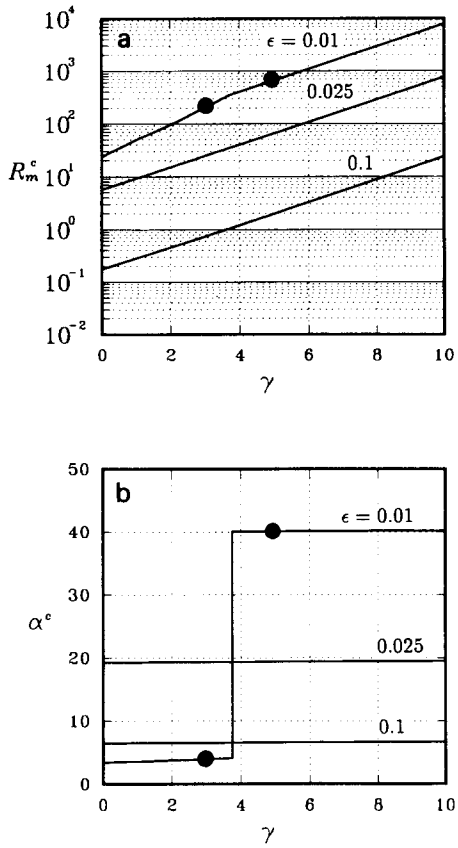

Fig. 3. Variations of (a) R_m^c and (b) α^c versus γ for various ϵ.

as we take $z = 0$ to be the position of the melt/mush interface, then $z = z^*$ accounts for the position of the top boundary of the stagnant lid in which no convection occurs due to the large viscosity. The onset of convection is therefore confined in the region $z^* < z < h$, where $z = h$ is the position of the top boundary of the solutal boundary-layer. In addition,

$$\Delta C_{z^*} = C_\infty - C|_{z=z^*} \tag{30}$$

accounts for the solute difference across the convection layer. Nondimensionalizing Eq. (30) yields

$$\Delta C_{z^*} = -\Delta C \Theta_b|_{z=z^*+h}, \tag{31}$$

where Θ_b is the dimensionless basic state concentration and can be expressed as [5]

$$\Theta_b|_{z=z^*} = \theta_i \exp(-z^*/\epsilon), \tag{32}$$

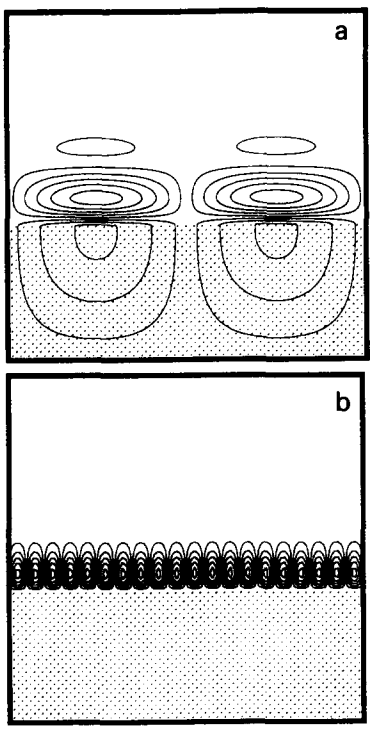

Fig. 4. Critical streamline pattern for the case of $\epsilon = 0.01$ as shown with solid circles in Fig. 3. (a) Mushy-layer mode convection, $\gamma = 3$, $R_m^c = 194.2$, $\alpha^c = 3.96$. (b) Boundary-layer mode convection, $\gamma = 5$, $R_m^c = 661.7$, $\alpha^c = 40.1$.

and

$$\theta_i = -\frac{\epsilon}{1-\epsilon}\theta_\infty \tag{33}$$

is the dimensionless basic state temperature at the melt/mush interface. The local viscosity ν_{z^*}, after nondimensionalizing and using the basic state temperature, can be expressed as

$$\nu_{z^*} = \nu_\infty \exp\left(\gamma^* e^{-z^*}\right), \tag{34a}$$

$$\gamma^* = \gamma\frac{\theta_\infty - \theta_i}{\theta_\infty - \theta_E}. \tag{34b}$$

Note that for the present analysis $\gamma^* \approx 0.5\gamma$. Accordingly, the local Rayleigh number can be written as

$$R_{loc} = \frac{-\beta^* g\Delta C H^3}{\kappa_{ll}\nu_\infty}\frac{\theta_i \exp(-z^*/\epsilon)}{\exp(\gamma^* e^{-z^*})}$$

$$= -(1+\mathcal{A})\mathcal{H}R_m\theta_i \exp\left(-\frac{z^*}{\epsilon} - \gamma^* e^{-z^*}\right). \tag{35}$$

When the onset of convection occurs, the convection must first take place in the region between the top of the stagnant lid ($z = z^*$) and the top boundary of the solutal boundary-layer with the largest possible R_{loc}. The maximum of R_{loc} can thus be obtained by

$$\frac{dR_{loc}}{dz^*} = -\frac{1}{\epsilon} + \gamma^* \exp(-z^*) = 0, \tag{36}$$

and thus

$$0 < \exp(-z^*) = \frac{1}{\gamma^*\epsilon} < 1, \tag{37}$$

since $0 < z^* < \infty$ and $0 < \exp(-z^*) < 1$. Eq. (37) yields

$$\frac{1}{\epsilon} < \gamma^*, \tag{38}$$

which is not relevant to the present analysis since we consider $0 \le \gamma^* \le 10$ while Eq. (38) implies that γ^* can be larger than 10^2 since $\epsilon \approx O(10^{-2})$. Accordingly, the maximum value of R_{loc} shall be $\max(R_{loc}|_{z=0}, R_{loc}|_{z=\infty})$. For $z = \infty$, $R_{loc} = 0$ is trivial. For $z = 0$,

$$R_{loc} = -\theta_i(1+\mathcal{A})\mathcal{H}\frac{R_m}{\exp(\gamma^*)} \propto \frac{R_m}{\exp(\gamma^*)}, \tag{39}$$

since the coefficient is a constant. Due to the fact that the critical local Rayleigh number is constant [11], the relation $\log(R_m^c) \propto \gamma^*$ accordingly holds. Note that the above scaling-analysis is valid for the boundary-layer mode convection, while a similar analysis can be made for the mushy-layer mode convection and the same conclusion can be reached.

We also consider the cases of different σ and $\mathcal{A}$. Fig. 5 illustrates the R_m^c and α^c for $\sigma = 0.1$, 1, 10, and 100. It is seen that the Prandtl number effect is insignificant, namely, the R_m^c for all σ considered are virtually the same and the α^c lies within the small range $19.3 < \alpha < 19.7$. The effect due to $\mathcal{A}$ is illustrated in Fig. 6, showing that the value of R_m^c is also hardly influenced by varying $\mathcal{A}$ while the α^c decreases as $\mathcal{A}$ increases. The linear relation between $\log(R_m^c)$ and γ holds in spite of varying σ and $\mathcal{A}$. The onset of convection is of the boundary-layer mode for above cases.

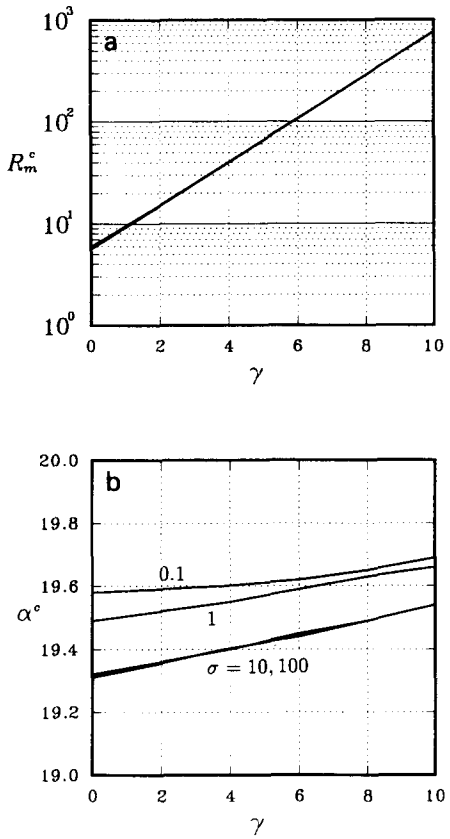

Fig. 5. Variations of (a) R_m^c and (b) α^c versus γ for various σ. Note that the curves in (a) for $\sigma = 0.1$, 1, 10 and 100 virtually overlap.

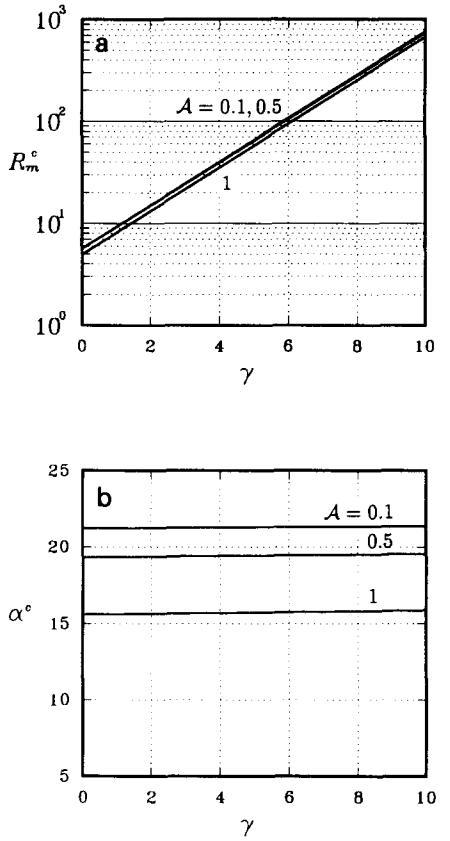

Fig. 6. Variations of (a) R_m^c and (b) α^c versus γ for various $\mathcal{A}$.

5. Discussion and conclusion

From above analysis it is shown that the effect on the double-diffusive convective stability due to the variation of σ and $\mathcal{A}$ is relatively insignificant compared with that due to ϵ. In particular, for small ϵ the onset of convection can change from the mushy-layer mode into the boundary-layer mode when γ increases. Moreover, as the mushy-layer mode convection prevails, the viscosity variation influences the stability more profoundly than as the boundary-layer mode convection predominates. For the metallic solution, the value of ϵ can be as low as 10^{-3}. According to the results shown in Fig. 3, we may infer that the onset of double-diffusive convection is generally of the mushy-layer mode in a wide range of γ whereas it will become the boundary-layer mode as γ is sufficiently large. Accordingly, the influence due to the viscosity variation in the metallic solution shall be much more significant than in the aqueous solution.

For both the mushy-layer mode and boundary-layer mode convections, the relation $\log(R_m^c) \propto \gamma$ holds, although the slope of the linear curve for the former mode is larger than for the latter (Fig. 3). This is because, as stated above, the effect of viscosity variation is larger to the mushy-layer mode than to the boundary-layer mode. In contrast to the thermal convection case in which the critical Rayleigh number increases linearly with γ, R_m^c increases exponentially with γ for the present double-diffusive system. The difference between these two systems emerges mainly from the driving mechanism of the instability, which is the thermal gradient for the thermal convection and is the solutal gradient for the double-diffusive convec-

tion. The characteristic length of the solutal boundary-layer is about $O(\epsilon)$ compared with that of the thermal boundary-layer. This significant difference in the characteristic length results in a different relation between the critical Rayleigh number and γ. The above speculation is supported by the results obtained by Lu [16], in which the similar aqueous solution unidirectionally solidifying from above is considered. In such a system, the onset of convection is a diffusive-type [17] double-diffusive convection (in contrast to the present salt-finger type), however, the results show that this convection is predominated by the thermal convection because its driving mechanism is the thermal gradient and the convection cell is of the size of the thermal boundary-layer thickness. As a result, we reached the conclusion that $R_m^c \propto \gamma$ holds, which is similar to the thermal convection case.

In summary, as the viscosity varies with temperature, the onset of convection is dramatically influenced by the viscosity contrast between the top and bottom fluids. For $\epsilon \leq 0.01$, the onset of convection is of the mushy-layer mode for small γ. As γ increases, the onset of convection becomes a boundary-layer mode due to the retardation of the flow by the high viscosity. For both modes of convection, the relation $\log(R_m^c) \propto \gamma$ holds, which is valid in a wide range of ϵ, σ, and $\mathcal{A}$, three major parameters determining the physical properties of the solution. For the metallic solution, the viscosity variation is particularly profound since the onset of convection in wide range of γ is of mushy-layer mode.

Acknowledgments

The financial support for this work from the Nation Science Council through Grant Nos. NSC 80-0401-E-002-26 and NSC 81-F-SP-002-04 is gratefully acknowledged.

References

[1] M. McLean, Directionally Solidified Materials for High Temperature Service (The Metals Society, London, 1983).
[2] S.M. Copley, A.F. Giamei, S.M. Johnson and M.F. Hornbecker, Met. Trans. 1 (1970) 2193.
[3] S. Tait and C. Jaupart, Nature 338 (1989) 571.
[4] C.F. Chen and F. Chen, J. Fluid Mech. 227 (1991) 567.
[5] M.G. Worster, J. Fluid Mech. 237 (1992) 649.
[6] F. Chen, J.W. Lu and T.L. Yang, J. Fluid Mech. 276 (1994) 163.
[7] G. Amberg and G.M. Homsy, J. Fluid Mech. 252 (1993) 79.
[8] D. Turnbull, Trans. Met. Soc. AIME 212 (1961) 422.
[9] H.R. Thresh and A.F. Crawley, Met. Trans. 1 (1970) 1531.
[10] K.C. Stengel, D.S. Oliver and J.R. Booker, J. Fluid Mech. 120 (1982) 411.
[11] M.K. Smith, J. Fluid Mech. 188 (1988) 547.
[12] S.R. Coriell, M.R. Cordes, W.J. Boettinger and R.F. Sekerka, J. Crystal Growth 49 (1980) 13.
[13] T.A. Litovitz, J. Chem. Phys. 20 (1952) 1088.
[14] R.J. O'Donnell and J.A. Zakarian, Ind. Eng. Chem. Process Design Develop. 23 (1984) 491.
[15] G.S. Beavers and D.D. Joseph, J. Fluid Mech. 30 (1967) 197.
[16] J.W. Lu, Convective instability in directional solidification of binary solutions, PhD Thesis, National Taiwan University, Taipei, Taiwan (1994).
[17] J.S. Turner, Buoyancy Effects in Fluids (Cambridge University Press, Cambridge, 1973).